

NACA RM A52I23



**NACA**

# RESEARCH MEMORANDUM

INSTRUMENTATION AND CALIBRATION TECHNIQUE FOR FLIGHT  
CALIBRATION OF ANGLE-OF-ATTACK SYSTEMS ON AIRCRAFT

By Norman M. McFadden, George R. Holden,  
and Jack W. Ratcliff

Ames Aeronautical Laboratory  
Moffett Field, Calif.

CLASSIFICATION CANCELLED

Authority NACA Res. Rep. Date 1-10-57

RN-111  
By 72B 1-30-57 See 1-2-57

CLASSIFIED DOCUMENT

This material contains information affecting the National Defense of the United States within the meaning of the espionage laws, Title 18, U.S.C., Secs. 793 and 794; the transmission or revelation of which in any manner to unauthorized person is prohibited by law.

**NATIONAL ADVISORY COMMITTEE  
FOR AERONAUTICS**

WASHINGTON NACA LIBRARY

December 5, 1952

LANGLEY AERONAUTICAL LABORATORY  
Langley Field, Va.

**CONFIDENTIAL**

## NATIONAL ADVISORY COMMITTEE FOR AERONAUTICS

RESEARCH MEMORANDUM

## INSTRUMENTATION AND CALIBRATION TECHNIQUE FOR FLIGHT

## CALIBRATION OF ANGLE-OF-ATTACK SYSTEMS ON AIRCRAFT

By Norman M. McFadden, George R. Holden,  
and Jack W. Ratcliff

## SUMMARY

Data are presented on the instrumentation and calibration technique used in determining the position error of angle-of-attack sensors mounted on the fuselage of a  $35^\circ$  swept-wing fighter airplane. The true angle of attack was determined by the use of a nose boom with five angle-of-attack vanes spaced 20 inches apart on alternate sides of the boom. Errors due to boom bending, upwash around the boom, and vane floating angle were measured and corrections applied to all indicated angles of attack. The position error at the forward vane was determined to be negligibly small.

## INTRODUCTION

In modern fire-control and guidance systems for aircraft and guided missiles it is necessary to use angle-of-attack and angle-of-sideslip signals. One promising method of obtaining these signals is by the use of flow-direction sensing devices mounted on the forward part of the fuselage. A calibration of the position error of such a device mounted on the fuselage of a  $35^\circ$  swept-wing fighter airplane has been made and reported in reference 1.

Since the release of <sup>this</sup> report much interest has been expressed in the calibration technique and instrumentation used in the investigation. The present report was prepared to give a description of the calibration technique and instrumentation used in obtaining the data of reference 1.

## NOTATION

M	Mach number
n	number of occurrences of each value of $\epsilon$
q	dynamic pressure $\left(\frac{1}{2} \rho V^2\right)$
R	distance from boom axis
R <sub>0</sub>	radius of boom
S	wing area, square feet
V	velocity, feet per second
V <sub>0</sub>	velocity in undisturbed stream, feet per second
C <sub>N</sub>	normal force coefficient $\left(\frac{\text{normal force}}{qS}\right)$
$\alpha_I$	indicated angle of attack, degrees
$\alpha_T$	true angle of attack, degrees
$\beta_T$	true sideslip angle, degrees
$\epsilon$	uncertainty or error of measurement
$\rho$	density, slugs per cubic foot
$\sigma$	standard deviation

## GENERAL METHOD OF CALIBRATION

To calibrate the position error of the fuselage detectors, it was necessary to compare the angle of attack indicated by the detectors with the true angle of attack of the airplane. The true angle of attack was obtained from the forward vane of a nose boom containing five vanes (fig. 1). To insure that the forward vane was in a region substantially free of the upwash field of the wings and fuselage, the local angle of attack at each vane location was plotted as a function of the distance of the vane from the front of the nose of the airplane. If the local angle of attack has reached an asymptotic value at the forward vane, the vane can be assumed to be out of the upwash field of the wings and fuselage.

$\frac{\alpha_I}{\alpha_T} = 1.04$   
for forward vane

The true local angle of attack at each vane location was obtained by adding corrections for vane floating angle, upwash around the boom, and boom bending to the indicated angles of attack. The corrections for upwash around the boom and for vane floating angle were obtained from calibrations of the nose boom made in the Ames 12-foot pressure wind tunnel. The corrections for boom bending were found by means of photographs of the boom taken during the test flights. To eliminate errors due to temperature effects on the voltage regulator and recording oscillograph, a flight calibration circuit was included in the instrumentation.

## EQUIPMENT AND INSTRUMENTATION

### Basic Airplane and Instruments

Test airplane.- The test airplane was a standard F-86A-5. Figure 2, the test airplane as instrumented for flight, and figure 3, a two-view drawing of the test airplane, show the nose boom with its five vanes, the location of the fuselage detectors, and the Kollsman head for the airspeed system mounted on the end of the nose boom.

Angle-of-attack vanes.- A nose boom, developed by North American Aviation, Inc. and modified by Naval Ordnance Test Station, Inyokern, was used to determine the true angle of attack. This boom contained five angle-of-attack vanes spaced 20 inches apart with the forward vane 100 inches in front of the nose of the airplane (figs. 1 through 3). The vanes themselves were wedges of approximately  $3^\circ$  of 0.70 aspect ratio. Potentiometer pickups were made of 600 to 650 turns of 0.001-inch wire wound on a 1/8-inch-diameter mandrel, 3/4-inch long. The wipers, attached directly to the shaft of the vanes, were made of 0.007-inch Paliney wire. Details of the angle-of-attack vanes are given in figure 4.

Fuselage detectors.- Specialties, Inc., Type J, Airstream Direction Detectors (known as ADD) were mounted as angle-of-attack detectors on the left and right sides of the fuselage about one-third root chord in front of the leading edge of the wing (see fig. 3). A third ADD mounted on the lower center line of the fuselage just behind the lip of the intake was used to measure sideslip. The ADD (fig. 5) is a self-actuating null-seeking device which operates on the difference in pressures at two slots  $60^\circ$  apart on a 3/8-inch cylindrical probe. The pressure difference at the two slots, operating on a paddle linked to the probe, rotates the probe until the pressures at the two slots are equal. A potentiometer is used to measure the angular rotation of the probe. A close-up of the sideslip probe is shown in figure 6.

Other instruments.- Standard NACA instruments were used to record impact pressure, static pressure, and normal acceleration. The impact and static pressures were obtained with a Kollsman-type airspeed head mounted on the nose boom 12-1/2 feet in front of the nose of the airplane. Reference 2 presents a calibration of a similar airspeed system on this airplane.

Angles indicated by the angle-of-attack vanes and the fuselage detectors were recorded on an 18-channel Consolidated oscillograph. The necessary power for the transducers was supplied from the airplane electrical system through a Sorensen regulated direct-current power supply set at 24 volts. A 0.1-second timer was used to synchronize records on all instruments installed in the airplane.

### Flight Calibrator

An in-flight calibration circuit was incorporated in the instrumentation to enable check calibrations of the recording circuits to be made in flight. This calibrator (fig. 7) consisted of a stepping switch actuated by the 0.1-second instrument timer which, at the beginning of each record, switched off the voltage supply to all recording circuits for 0.2-second (calibration point number 1); then switched each channel to a fixed potentiometer for another 0.2 second (calibration point number 2); and finally, switched each channel to its normal recording potentiometer. This produced a two-point check calibration which was used to correct the calibration of each channel for each record (table I). More recent installations have used motor driven switches and placed the calibration at the end rather than at the beginning of the record.

### CALIBRATION TECHNIQUE

#### Angle-of-Attack Vanes

Besides the corrections required to correct for the electrical eccentricities of the recording circuits as determined by flight calibration, it was necessary to correct the indicated angles of attack for errors due to bending of the angle-of-attack boom, upwash around the boom, and for the floating angle of the angle-of-attack vanes. Corrections for boom bending were obtained from photographs of the tip of the boom taken in flight, using a gunsight camera mounted in the lower lip of the intake. Prior to flight, the angular rotation of the boom axis at the base of each vane was measured and the corresponding displacement

on the photograph of the tip of the boom was evaluated with the boom subjected to a uniformly distributed load.

The effects of upwash around the boom and the floating angle of the angle-of-attack vanes were obtained from tests in the Ames 12-foot pressure wind tunnel over a Mach number range of 0.50 to 0.96 at several tunnel total pressures and in both the upright and inverted positions. Figure 8 shows the angle of attack indicated by the forward vane as a function of true angle of attack for both the right side up and inverted positions. The floating angle (one-half the difference between the right side up and inverted indications of the angle-of-attack vane) is relatively independent of Mach number and equal to  $0.35^\circ$  to  $0.40^\circ$ . The data of a Mach number of 0.96 are considered to be unreliable because of tunnel choking. Similar data were obtained for the other four vanes.

The deviation of the lines of figure 8 from the  $45^\circ$ , or slope of 1, is due to the bending of the boom under air loads and to the upwash around the boom. To separate these effects, the slope ( $d\alpha_I/d\alpha_T$ ) is plotted in figure 9 as a function of the tunnel dynamic pressure and the resulting curve extrapolated to zero dynamic pressure. The value of the intercept,  $d\alpha_I/d\alpha_T = 1.058$ , at zero dynamic pressure (hence zero boom bending due to aerodynamic loads) is the measure of the upwash effect. The slope of the line in figure 9 could be used to determine the boom bending due to dynamic pressure; however, since the flight data were affected by acceleration as well as by dynamic pressure, the flight data were corrected from pictures taken of the boom in flight as discussed previously.

Considerations of two-dimensional incompressible flow about a circular cylinder (reference 3) indicate that

$$V = V_0 \left[ 1 + \left( \frac{R_0}{R} \right)^2 \right]$$

on the plane through the center of the cylinder and perpendicular to the flow. Assuming independence of the cross flow, it follows that for small angles

$$\alpha_I = \alpha_T \left[ 1 + \left( \frac{R_0}{R} \right)^2 \right]$$

The ratio  $\alpha_I/\alpha_T$  as a function of  $R/R_0$  is plotted in figure 10. The circled point, the one test point for the vane-boom configuration of this report, indicates good agreement with the simple theory.

An alternate method of obtaining the floating angle of the vanes is to fly on successive flights with the boom rotated  $180^\circ$ , thus using the angle-of-attack vanes both right side up and inverted. Figure 11 shows the angle of attack indicated by the forward vane both right side up and inverted as a function of the angle of attack indicated by the right

fuselage detector. The agreement with the tunnel results is quite good, the flight results indicating the floating angle to be about  $0.40^\circ$  to  $0.45^\circ$ .

We can now correct the angle of attack indicated by each vane for vane floating angle, upwash around the boom, and boom bending to give the correct value of the local flow angle. To obtain the true angle of attack of the airplane, the corrected local angle of attack at each vane position is plotted as a function of its distance in front of the nose of the airplane. This is done in figure 12 for several normal force coefficients at a Mach number of 0.81 and at several Mach numbers over a normal force coefficient range of 0.17 to 0.35. (Data for the vane 80 inches forward of the nose are omitted because of instrument malfunction.) This shows that the vane 60 inches forward of the nose of the airplane is substantially free of position error and the vane 100 inches forward of the nose is certainly (for practical purposes) out of the influence of the fuselage and wing. Consequently, this forward vane was used as indicating the true angle of attack without applying corrections for position error.

To give an idea of the relative importance of the various corrections that were applied to the angle-of-attack vane indications, a tabulation of the maximum correction applied in each case is given below:

<u>Correction</u>	<u>Maximum value</u>
Vane floating angle	$0.45^\circ$ (vane at 60 in.)
Boom bending	$1.25^\circ$
Upwash around boom	$0.62^\circ$
Flight calibrator	$0.75^\circ$
Position error	$0.0^\circ$

Associated with the use of numerous corrections, a rather careful calibration technique was found necessary to keep the accuracy of the data within acceptable limits. Prior to the series of flights a calibration was made of the angle of attack of the vane as a function of the oscillograph-trace deflection using the calibration fixtures shown in figure 13. The zero was established by the zeroing jig (merely a channel with the legs ground parallel so that when placed against the boom and the shaft of the vane the vane will be held parallel to the boom). The calibration was taken in  $2^\circ$  increments, for both increasing and decreasing angle of attack, taking care to always approach the desired value from below when increasing angle of attack and from above when decreasing angle of attack to bring out any hysteresis that might be present. Just prior to and just after each flight a check calibration was taken of  $0^\circ$ ,  $+5^\circ$ , and  $+10^\circ$ . These pre- and post-flight check calibrations occasionally revealed a small zero shift which was applied

to the calibration before working up the data. During this calibration procedure the flight calibrator was operating and all calibration points were shifted in accordance with its indications. Table I is the computation sheet used to correct the data points for the zero and slope shifts of the recording circuits as measured with the flight calibrator.

### Fuselage Detectors

There is no provision for directly checking the alinement of the ADD probe with the fuselage reference line. It is necessary to rely upon the initial adjustment by the manufacturer in which two jig holes (fig. 5) are established perpendicular to the air stream when the wiper is in the center of the potentiometer. By use of a fixture in the jig holes and a gunner's quadrant (an inclinometer), the instrument was alined with the fuselage reference line. Then calibrations of the probe were made by clamping the calibration fixture shown in figure 13 to the probe, securing a pointer to the fuselage, and using the clockwise stop of the instrument as a reference point. (The angular displacement of the probe from the clockwise stop to its position when the wiper was in the center of the potentiometer was previously determined in the laboratory.) As in the case of the angle-of-attack vane calibrations, the ADD calibrations were made in  $2^\circ$  increments, both increasing and decreasing angle of attack.

As a check on the accuracy with which the jig holes in the instrument were alined, the two angle-of-attack ADD's were interchanged, thus inverting them from their original position. Figure 14 presents the normal force coefficient as a function of the angle of attack indicated by the two ADD's for both the upright and inverted positions. The two curves for ADD number 13 fall on one another, while number 23 indicates an angle of attack  $0.4^\circ$  larger when on the left side of the fuselage and  $0.4^\circ$  smaller when on the right side of the fuselage, showing that instrument number 13 was properly alined, while number 23 was out of alinement by  $0.4^\circ$ .

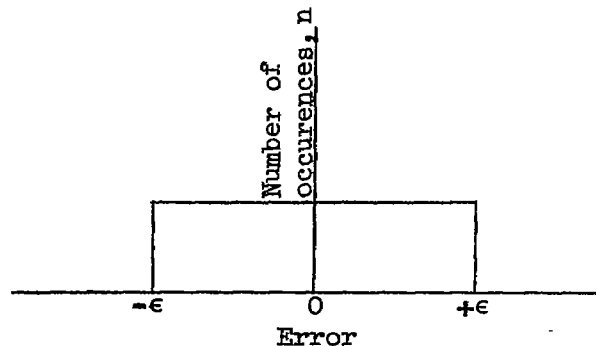
### Accuracy of Measurement

Angle-of-attack vanes.— There are certain difficulties in establishing the over-all accuracy of a measurement where there are several corrections involved, each of which in itself is subject to error. The uncertainties of each component of the final corrected measurement can be estimated with a fair degree of confidence. However, a simple summation of these uncertainties, although giving a maximum possible error which would not be expected to be exceeded, would give a value



which could be expected to be approached only very rarely. A more realistic approach is to obtain the standard deviation of the final measurement from the standard deviations of each component measurement.

In estimating the uncertainties of the various components of the angle-of-attack measurement, most of the uncertainties were of the order of one or two times the least count of the measuring instrument involved. In the case where the uncertainty is entirely within the least count of the instrument, there would be an equal probability of the true value lying anywhere within the region of uncertainty, or, in other words, the error distribution would be a rectangle as shown below:



The standard deviation, defined as the square root of the mean of the squared deviations, in this case would be

$$\sigma = \left( \frac{\int_{-\epsilon}^{\epsilon} nx^2 dx}{2n\epsilon} \right)^{1/2} = \frac{\epsilon}{\sqrt{3}}$$

Assuming this type of distribution for all errors (a conservative assumption), and since the standard deviation of the final corrected measurement is the square root of the sum of the squares of the individual standard deviations (reference 4), the standard deviation of the final measurement is

$$\sigma_{\text{total}} = \sqrt{\sum \sigma^2} = \frac{1}{\sqrt{3}} \sqrt{\sum \epsilon^2}$$

In this case, for a large number of observations the errors would be less than the standard deviation 58 percent of the time.

Estimates of the uncertainties of each component of the final measurement of the true angle of attack are given in the following tabulation:

Basic calibration.....	$\pm 0.10^\circ$
Flight calibration.....	$\pm 0.10^\circ$
Pre- and post-flight zeros....	$\pm 0.05^\circ$
Boom upwash correction.....	$\pm 0.05^\circ$
Floating angle correction.....	$\pm 0.05^\circ$
Boom bending.....	$\pm 0.05^\circ$

$$\text{Standard deviation, } \sigma = \sqrt{\sum \epsilon^2} / \sqrt{3} = 0.10^\circ$$

There is an additional possible source of error from assuming the upwash effect of the wings and fuselage to be negligible for the forward vane. This error would be proportional to the angle of attack and, from figure 12, it would appear that errors from this source would be less than  $0.05^\circ$ .

Fuselage detectors.- An analysis of the torque theoretically available and measurements of the static friction of the ADD indicates its sensitivity to be  $0.11^\circ$  at the minimum values of dynamic pressure encountered during the tests. The resolution of the recording circuits of the ADD is much better than this value.

#### TEST FLIGHTS

The test flights consisted of a series of wind-up turns, increasing acceleration up to the buffet boundary while holding zero sideslip and Mach number as constant as possible. It is particularly necessary to maintain the sideslip angle near zero, for, as shown in figure 15, the angle of attack indicated by the fuselage detectors is a function of sideslip. The desired calibration is obtained by comparing the true angle of attack with that indicated by the fuselage detectors. As a sample of the data in the final form, figure 16 presents the data for 35,000 feet at several Mach numbers. Over 80 percent of all data points taken are within  $\pm 0.1^\circ$  of the faired straight lines, while over 96 percent are within  $\pm 0.25^\circ$ . (See reference 1 for complete data and discussion of results.)

A computation sheet showing the method of reduction of the angle-of-attack data to the final form is presented in table II.

## CONCLUDING REMARKS

With the angle-of-attack vane installation described in this report, the true angle of attack was measured with the standard deviation of the random errors estimated to be  $\pm 0.10^\circ$ . In addition there was a consistent error proportional to angle of attack which was estimated to be less than  $0.05^\circ$  at the maximum values of angle of attack encountered. This accuracy was obtained by measuring the effects of and applying corrections for upwash around the boom, vane floating angle, and boom bending. The position error (upwash from the fuselage and wings) was measured and found to be negligibly small at the position of the forward vane (100 inches in front of the nose of the airplane).

The vane floating angle and boom upwash corrections were obtained by the use of wind-tunnel calibrations. However, it was shown that the vane floating angle could be obtained in flight by a  $180^\circ$  rotation of the boom on which the angle-of-attack vanes were mounted, and that simple theoretical estimates of the boom upwash were quite good. Therefore, it should be possible to make a similar calibration without recourse to wind-tunnel tests. However, if the vanes are much closer to the center of the boom than two boom diameters (distance of this test), the theoretical corrections become quite large and further checks of the upwash around the boom should be made.

In this investigation the airplane angle of attack was related to a local flow angle measured on the fuselage. Any sensing device of suitable sensitivity and accuracy could be used to measure this local angle.

Ames Aeronautical Laboratory  
National Advisory Committee for Aeronautics  
Moffett Field, California

## REFERENCES

1. McFadden, Norman M., Rathert, George A., Jr., and Bray, Richard S.: Flight Calibration of Angle-of-Attack and Sideslip Detectors on the Fuselage of a  $35^\circ$  Swept-Wing Fighter Airplane. NACA RM A52A04, 1952.
2. Thompson, Jim Rogers, Bray, Richard S., and Cooper, George E.: Flight Calibration of Four Airspeed Systems on a Swept-Wing Airplane at Mach Numbers up to 1.04 by the NACA Radar-Phototheodolite Method. NACA RM A50H24, 1950.

3. Glauert, Hermann: The Elements of Aerofoil and Airscrew Theory. The MacMillan Co., New York, 1943, p. 30.
4. Cramér, Harald: Mathematical Methods of Statistics. Princeton University Press, 1946.

TABLE I.- CALCULATION SHEET TO CORRECT MEASURED TRACE DEFLECTION FOR SENSITIVITY AND ZERO SHIFTS OF RECORDING CIRCUITS AS INDICATED BY THE FLIGHT CALIBRATOR

1	2	3	4	5	6	7	8	9	10	11	12	13	14
Run No.	Trace deflection measured from reference line in inches					(2)-(5)	(4)-(3)	(6)-(5)	(8)÷(9)	(10)×(7)	(11)÷(5)	(3)-(5)	(12)÷(13)
	Record trace	Calibration point #1 Basic galv. zero	Calibration point #2	Calibration point #1 Recorded galv. zero	Calibration point #2 Recorded calib.	Galv. deflection	Basic sensitivity (slope)	Recorded sensitivity (slope)	Sensitivity ratio	Galv. deflection corrected for sensitivity	Trace deflection corrected for sensitivity	Galv. zero shift	Trace deflection corrected for sensitivity and zero shift
1	5.830	.690	2.920	.890	3.070	4.940	2.230	2.180	1.022	5.050	5.940	-.200	5.740



TABLE II.- CALCULATION SHEET TO REDUCE FILM RECORDS TO TRUE LOCAL ANGLE OF ATTACK  
FOR  $\alpha$  VANES AND TO ANGLE OF ATTACK INDICATED BY THE ADD

1	2	3	4	5	6	7	8	9	10
Run No.	Angle-of-attack vane							ADD	
	Corrected trace deflection Column (1) table I for angle-of- attack record	Angle of attack, degrees. Column (2) + calibration curve	Boom deflection in photograph, inches	$\Delta \alpha$ , degrees. Column (4) + calibration curve	$\alpha$ corrected for boom deflection. Column (3) + (5)	$\alpha$ corrected for boom deflection and upwash around boom. Column (6) $\times 1.058$	True local angle of attack. Column (7) - vane floating angle	Trace deflection Column (4) table I for ADD record	Angle of attack indicated by ADD Column (9) + calibration curve
1	5.74	-.43	.09	.48	.05	.05	-.30	5.08	-1.05

NACA

~~CONFIDENTIAL~~

NACA RM A52I23

~~CONFIDENTIAL~~

~~CONFIDENTIAL~~

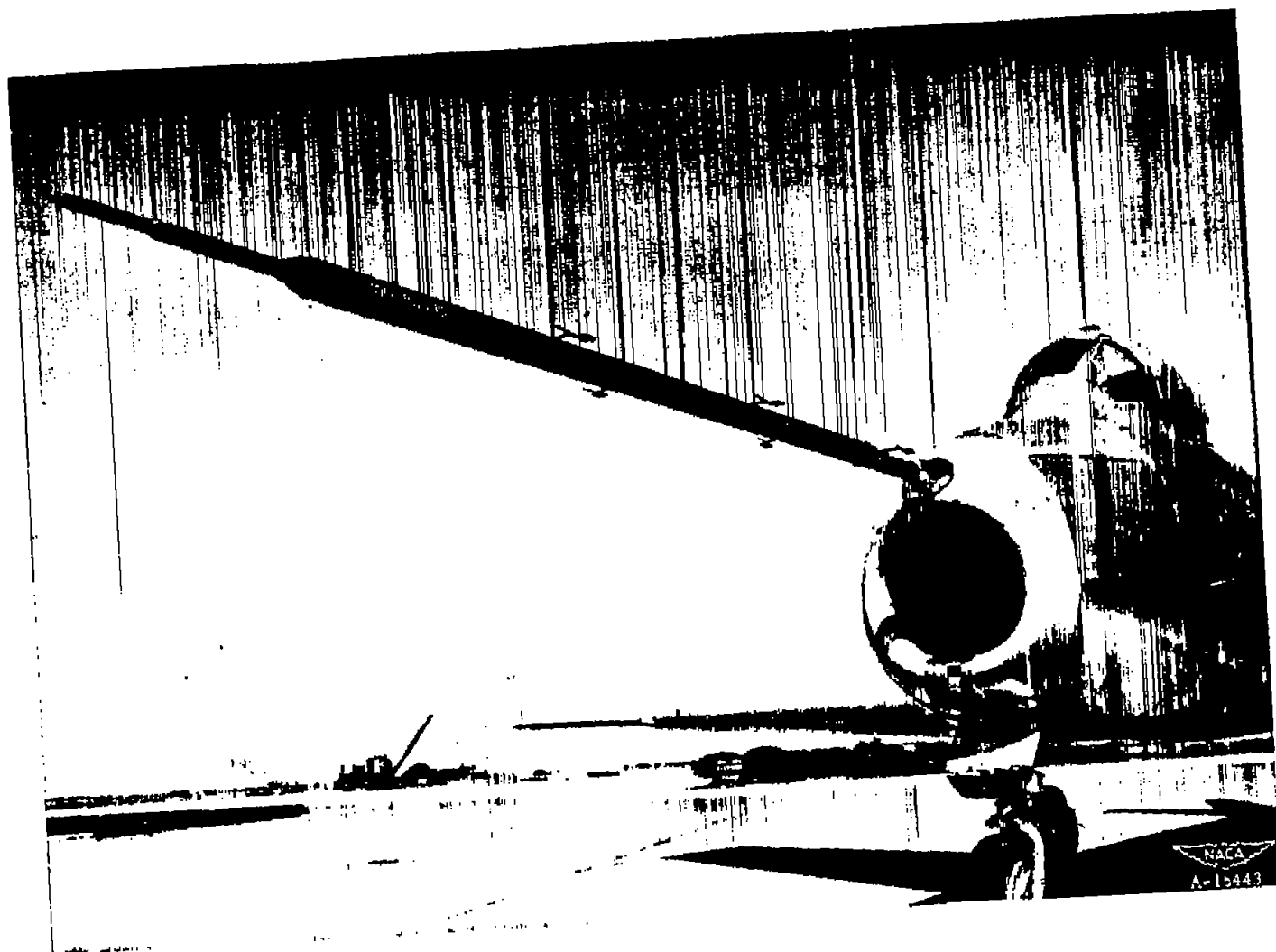


Figure 1.- The angle-of attack vane and nose-boom installation.



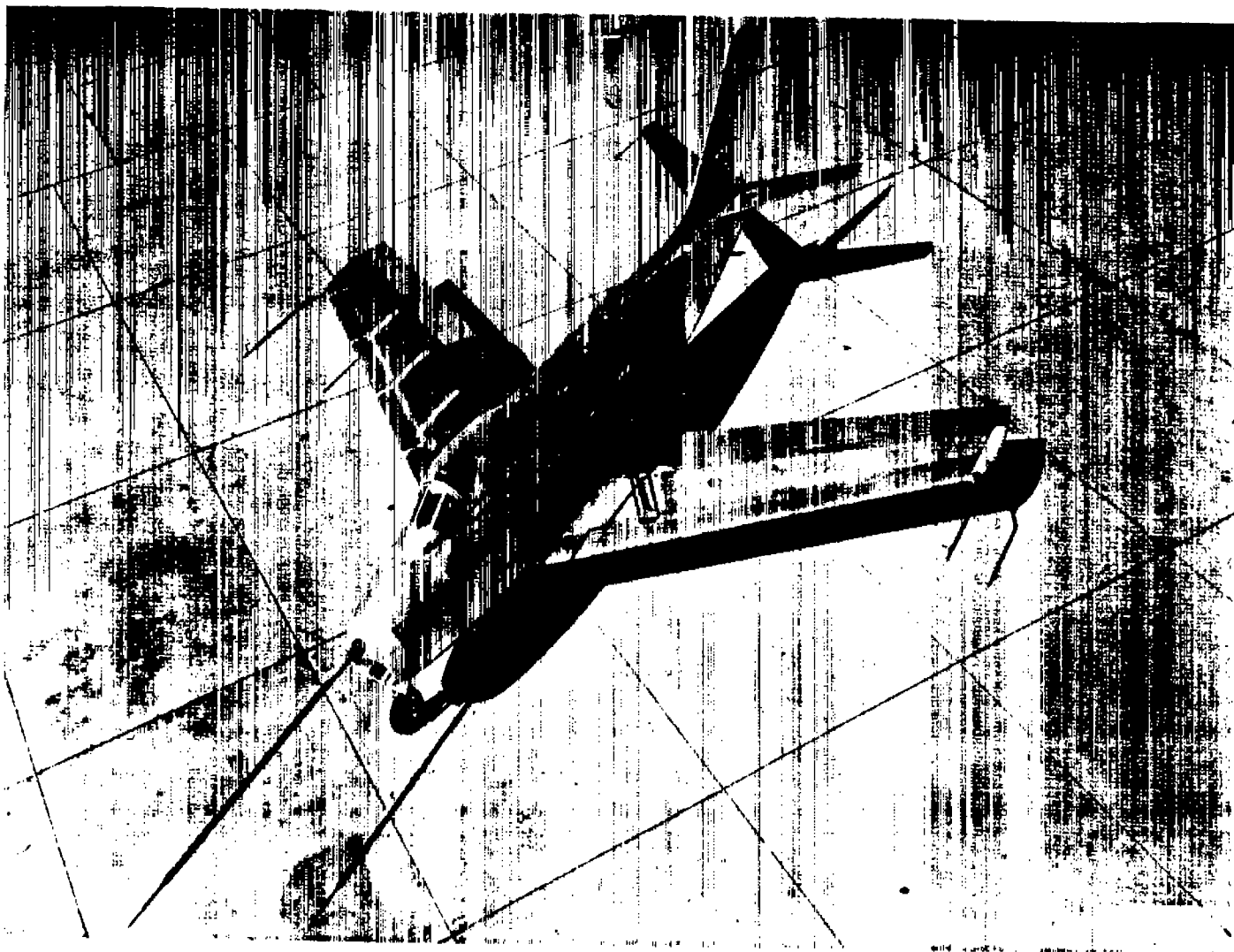


Figure 2.- The test airplane.

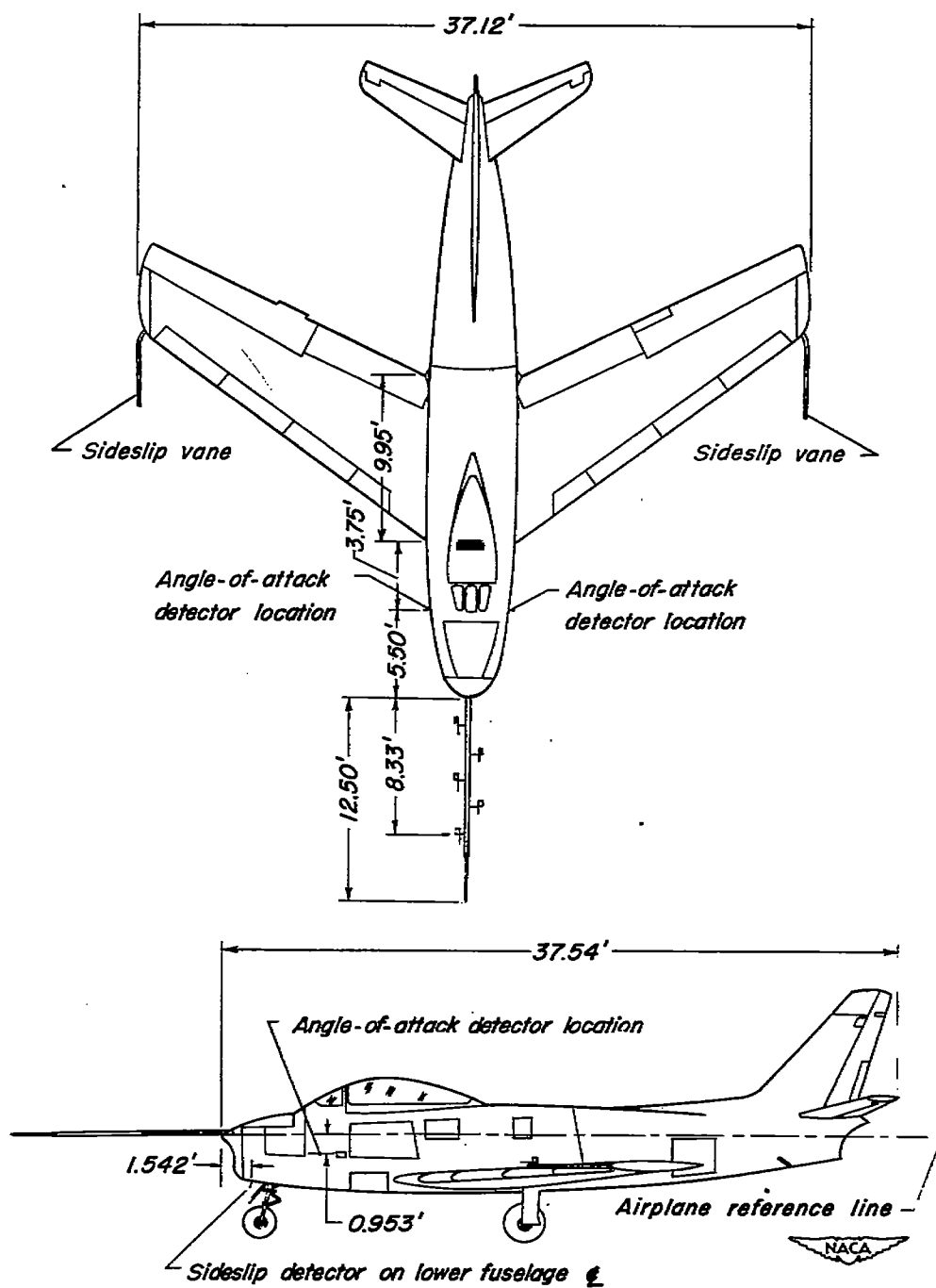


Figure 3.-Two-view drawing of the test airplane.

Note:  
All dimensions in inches

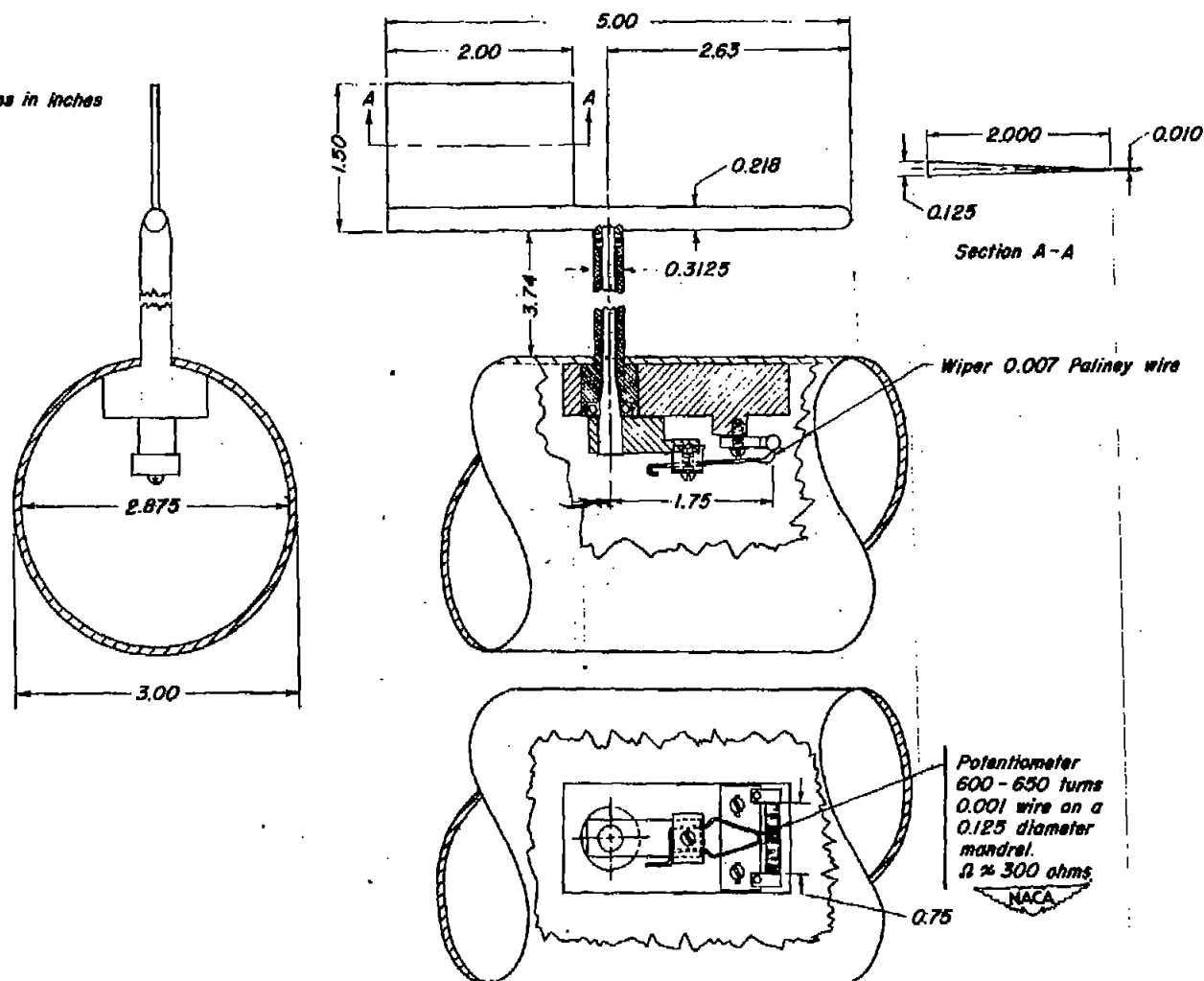


Figure 4.- Angle of attack vane and potentiometer pickup.

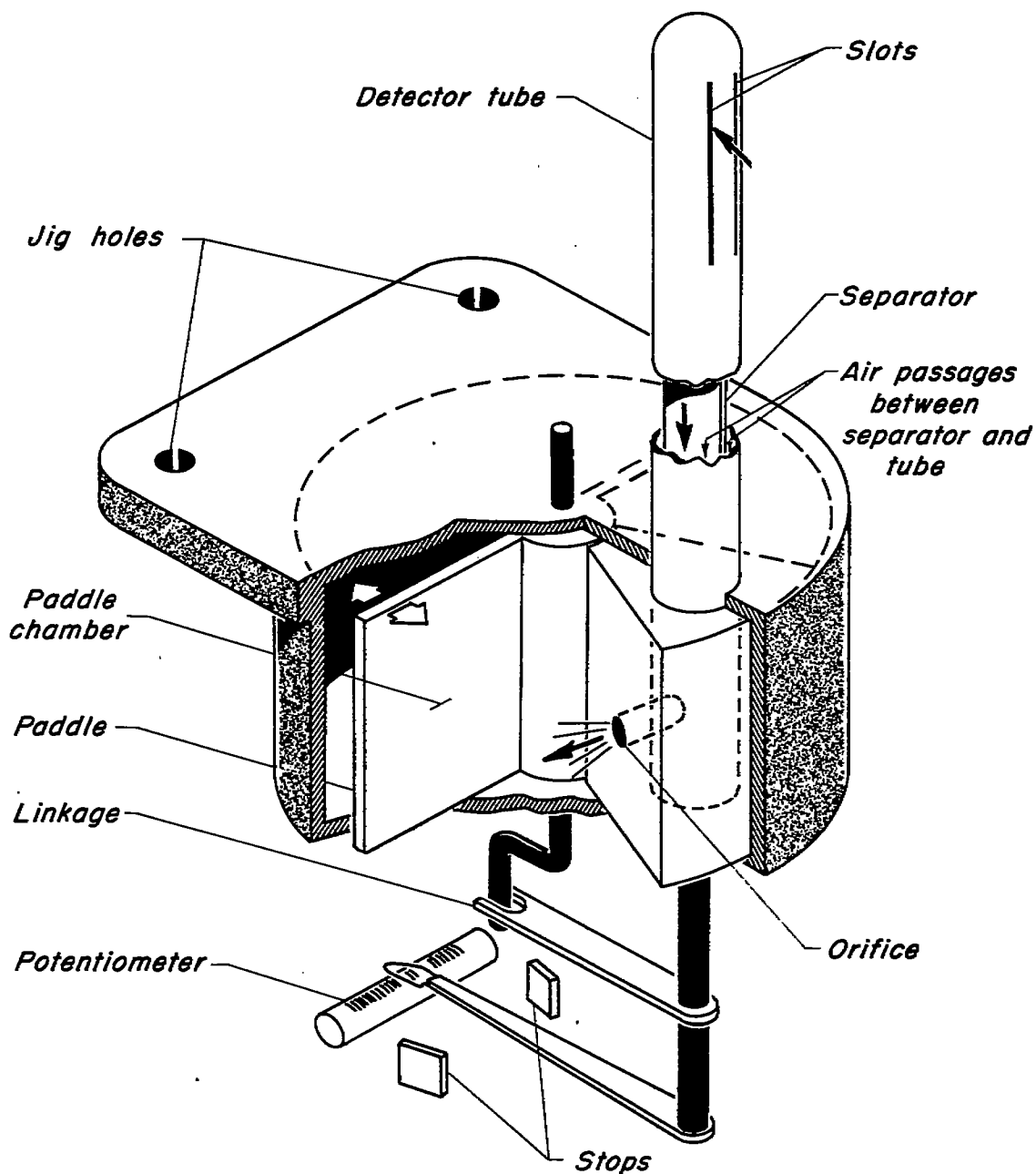


Figure 5.- Schematic drawing of the Specialties Incorporated,  
Airstream Direction Detector.



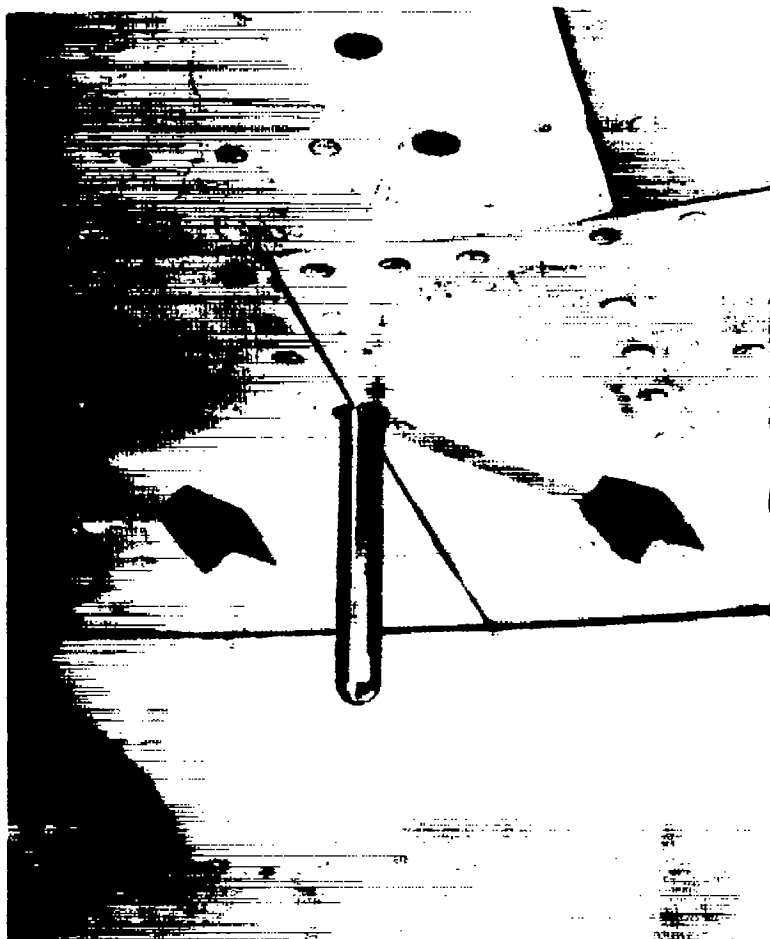


Figure 6.— Probe of the sideslip fuselage detector.

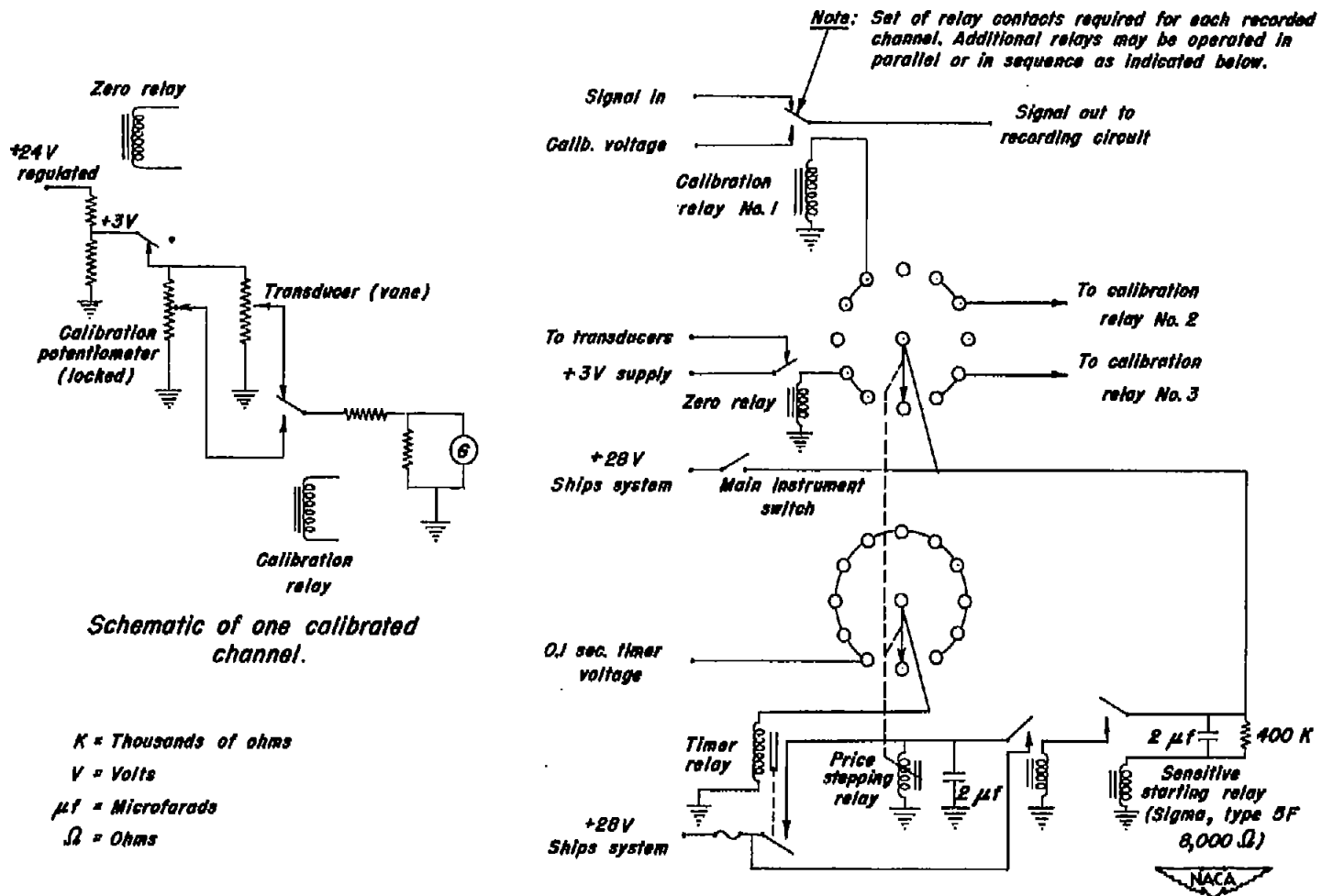


Figure 7.- Schematic of flight calibrator circuit.

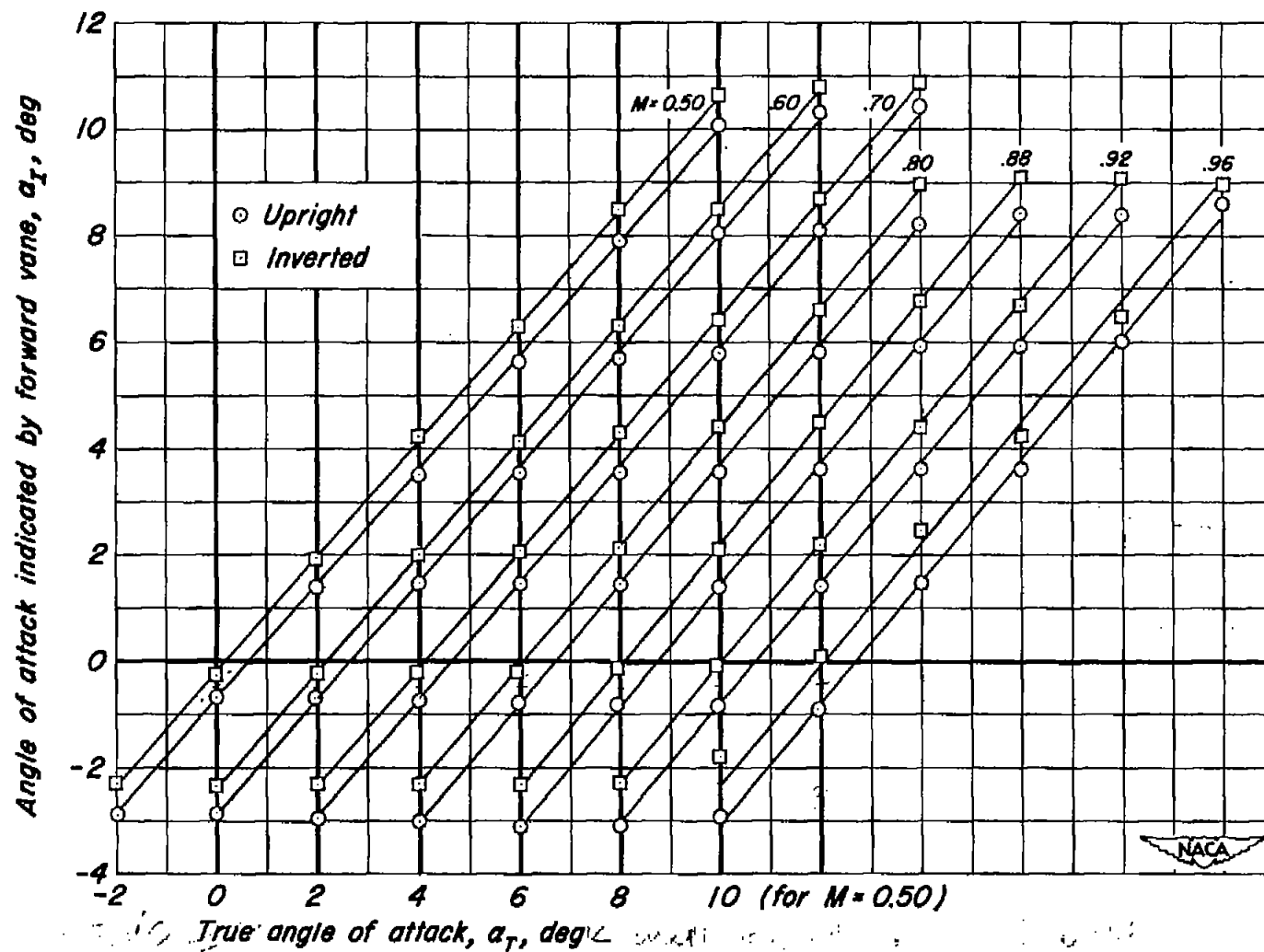
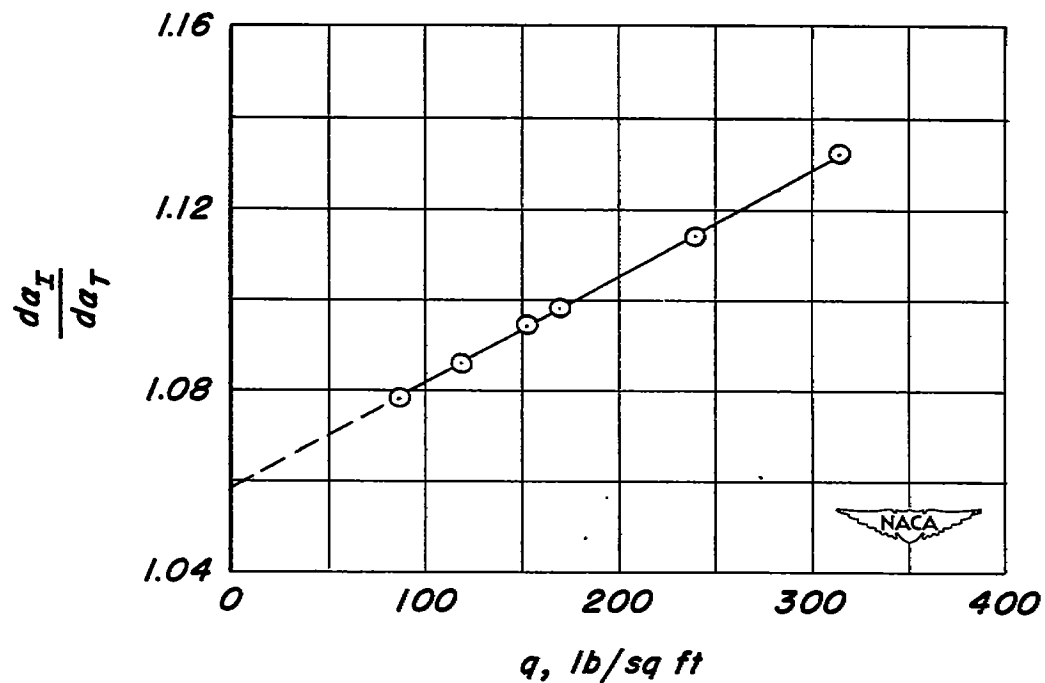


Figure 8.-Typical variation of the angle of attack indicated by the nose-boom vanes with true angle of attack at various Mach numbers, forward vane. Ames 12-foot pressure-wind-tunnel tests.



**Figure 9.**— The variation with dynamic pressure of the rate of change of the angle of attack indicated by the forward vane of the nose boom with the true angle of attack as measured in the Ames 12-foot pressure wind tunnel.



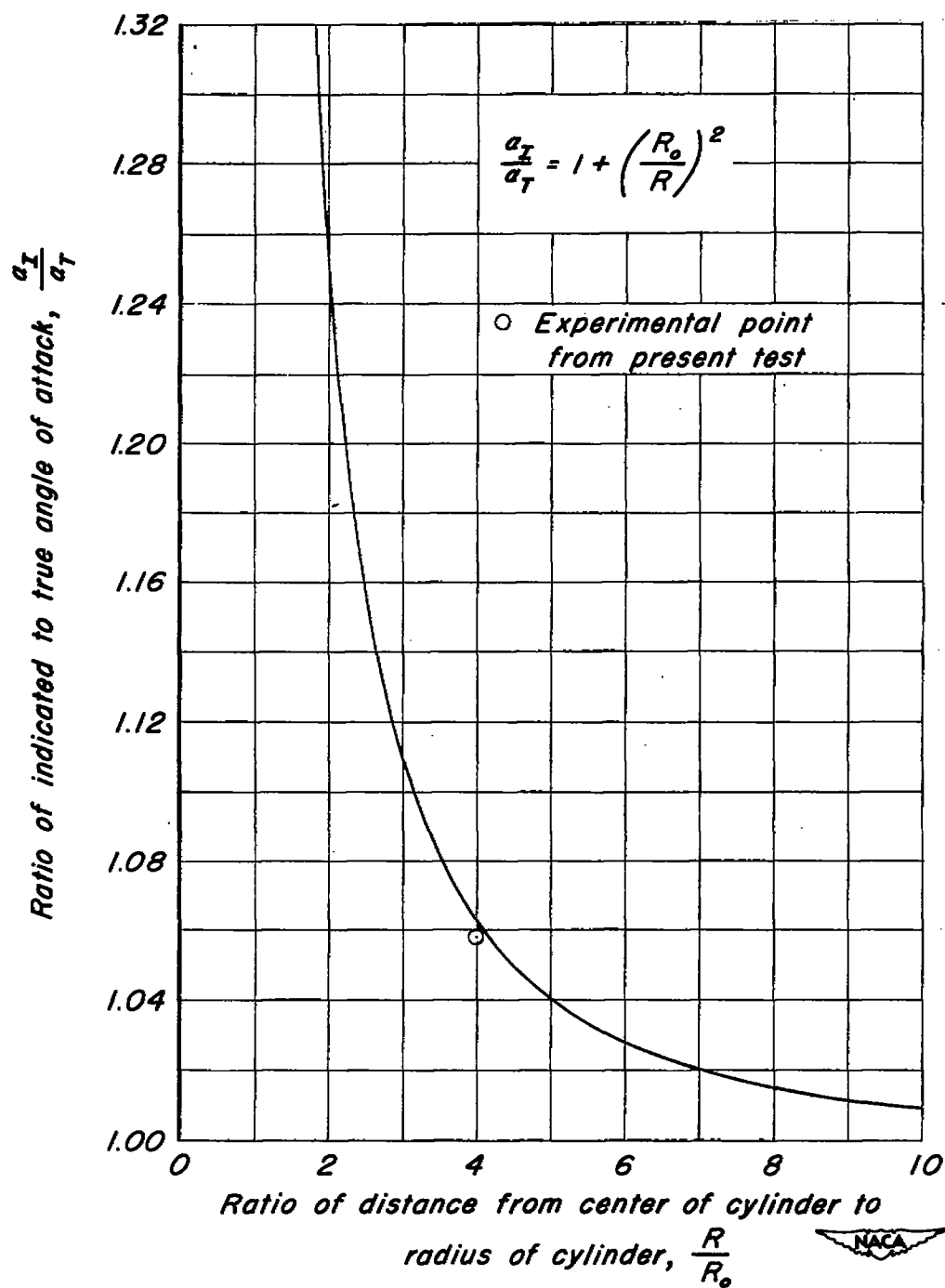


Figure 10.—Upwash around cylinder.

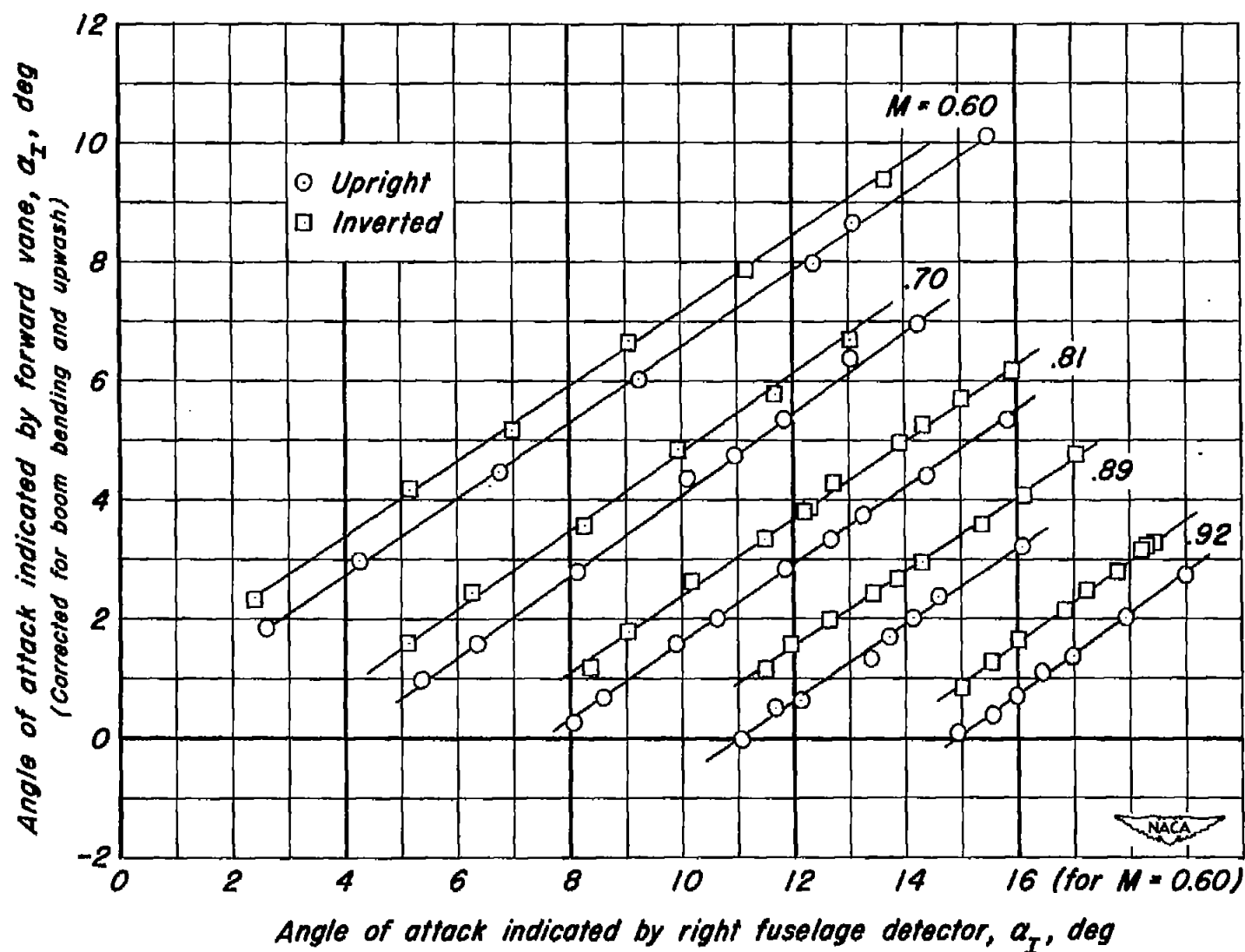
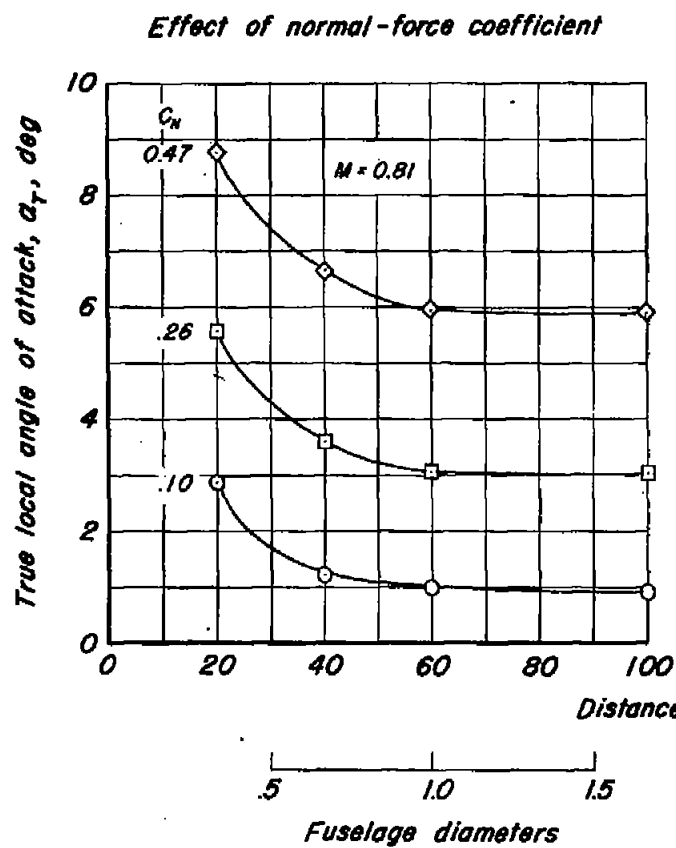


Figure 11.—The variation of the angle of attack indicated by the forward angle-of-attack vane in both the upright and inverted positions with the angle of attack indicated by the right fuselage detector in flight.



**Effect of Mach number and normal-force coefficient**

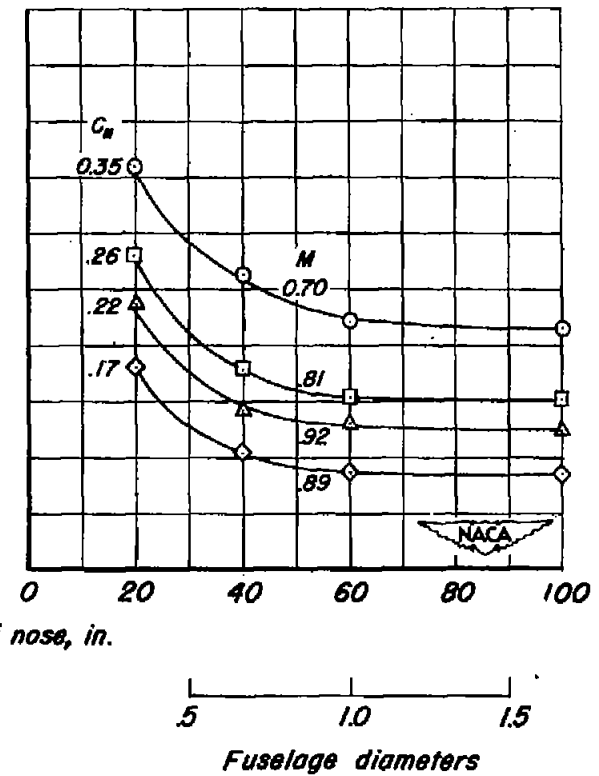


Figure 12.—Variation of local angle of attack with distance in front of nose of airplane.

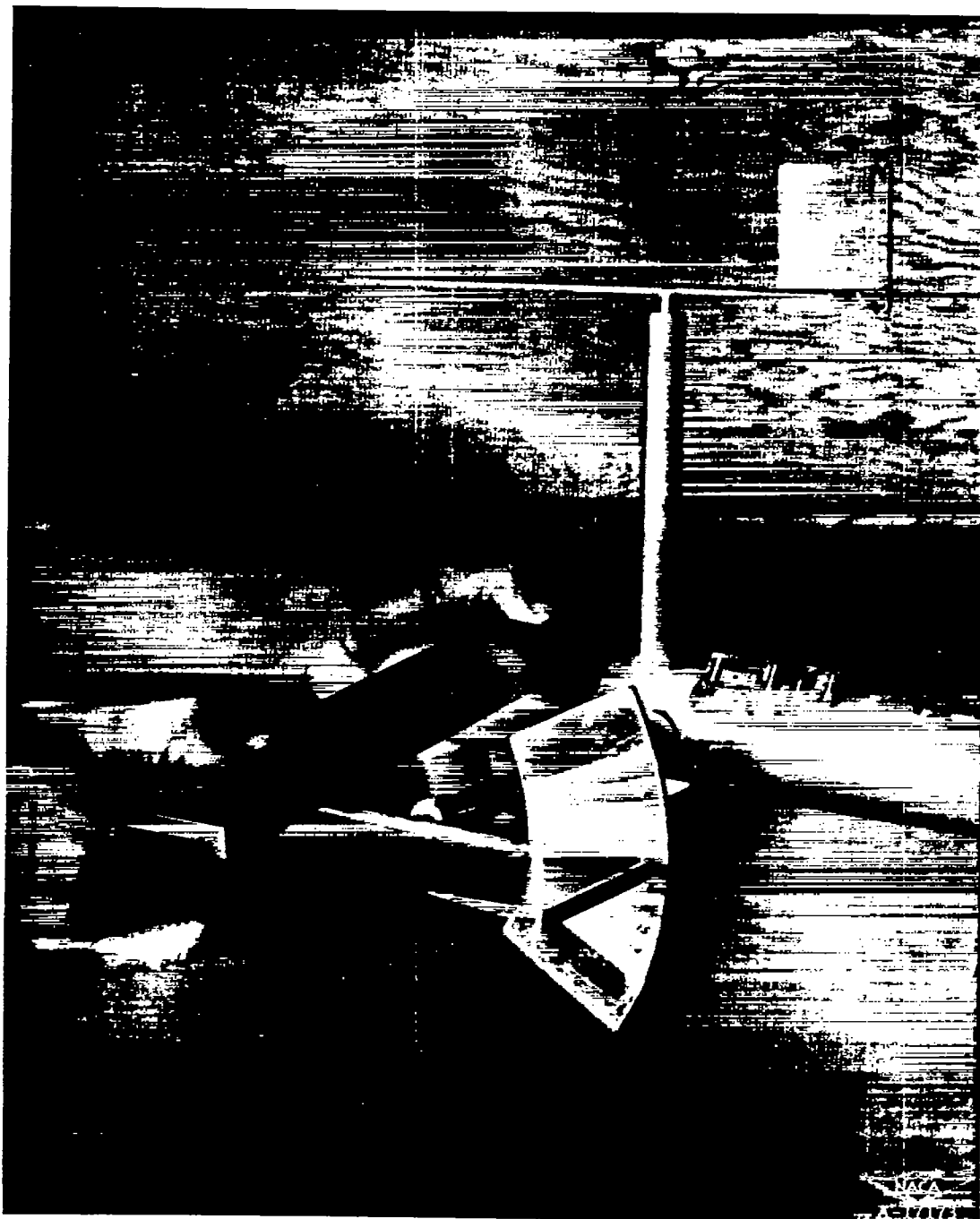


Figure 13.— Calibration fixture and zeroing jig in use.



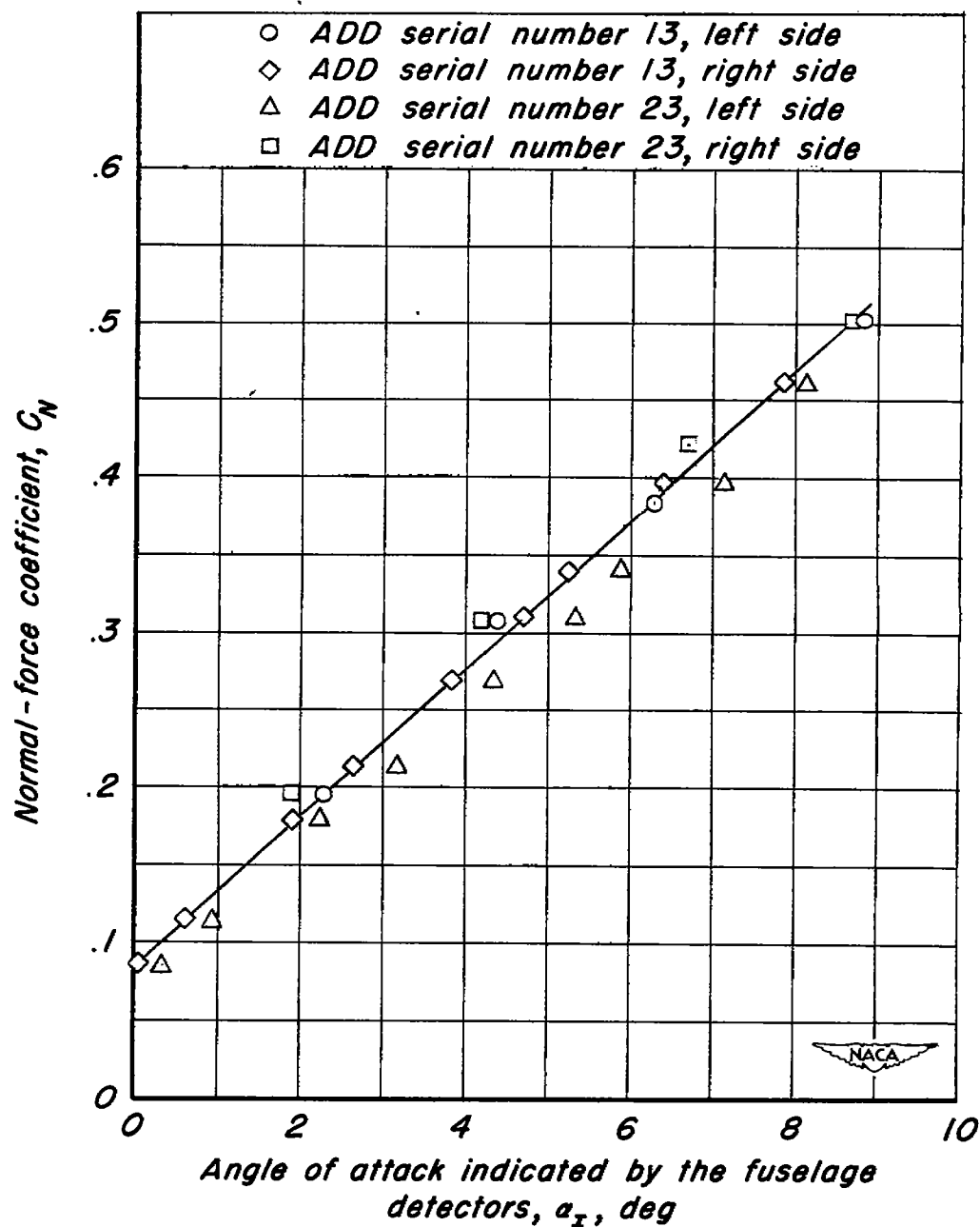


Figure 14.-The variation of normal-force coefficient with angle of attack indicated by the fuselage detectors in normal position and interchanged.

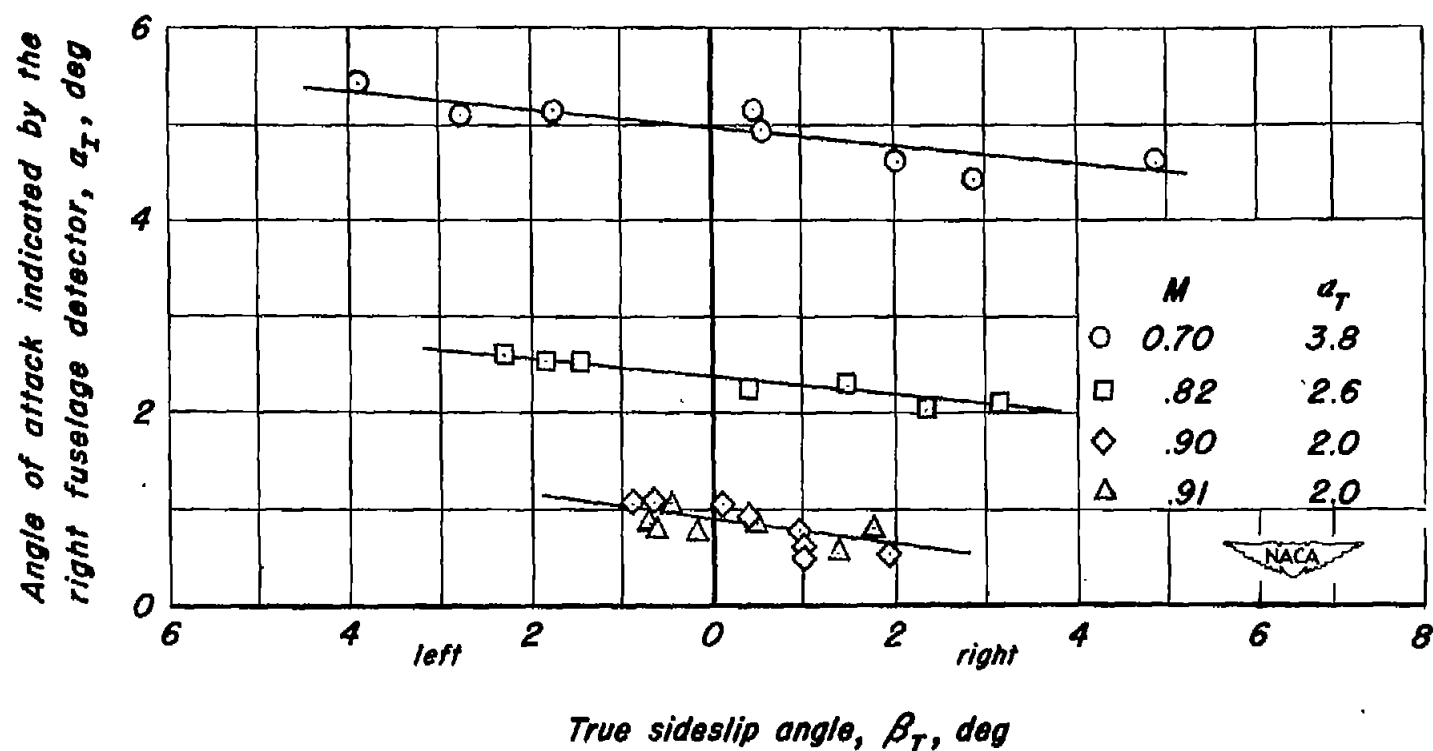


Figure 15.—The effect of sideslip on the angle of attack indicated by the right detector for several values of Mach number and at constant angles of attack.

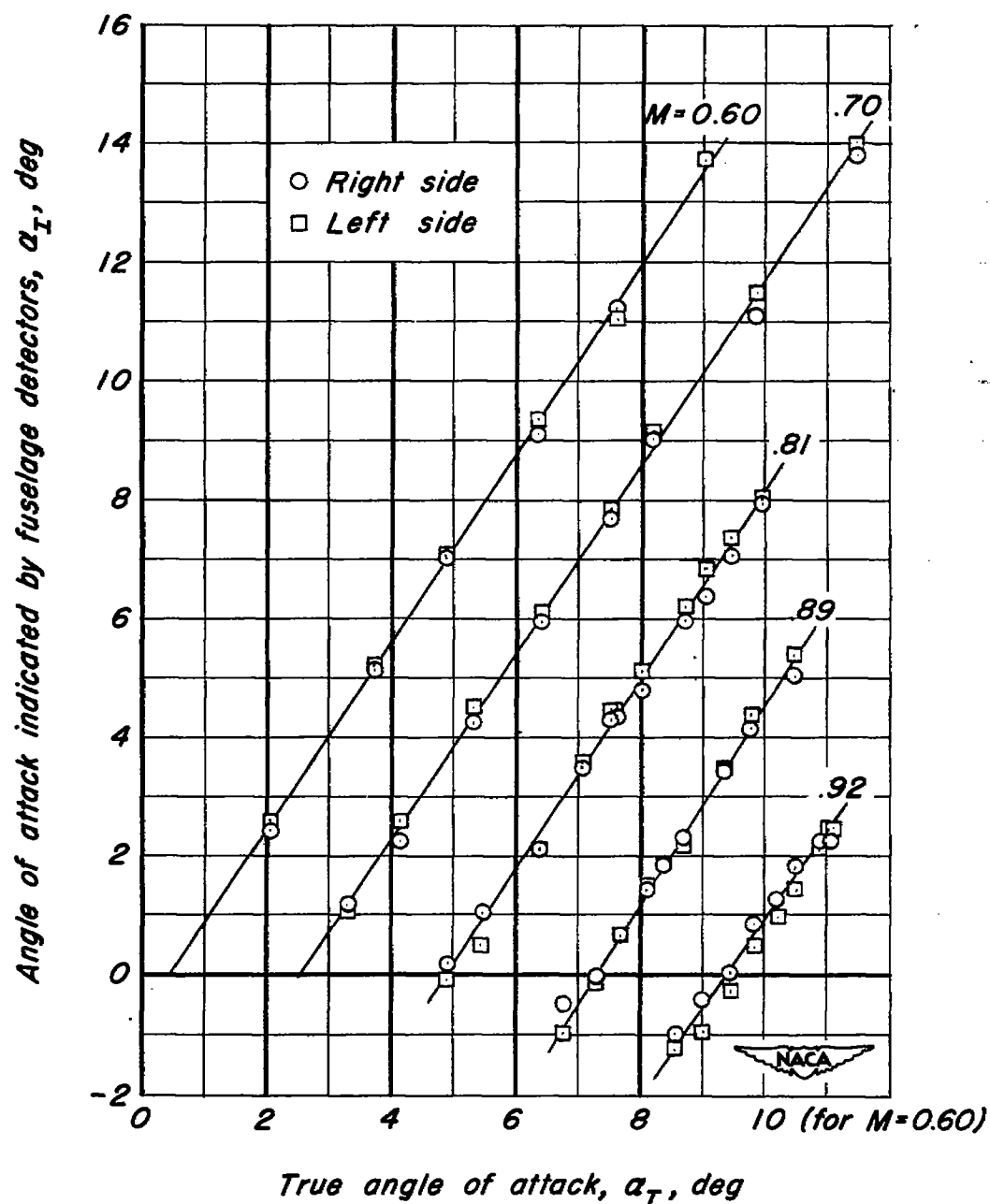


Figure 16.—The variation of indicated angle of attack with true angle of attack at several Mach numbers and 35,000 feet altitude.

SECURITY INFORMATION

~~CONFIDENTIAL~~

~~CONFIDENTIAL~~